
# High-Entropy Mixtures of Pristine Fullerenes for Solution-Processed Transistors and Solar Cells

# High-entropy mixtures of pristine fullerenes for solution-processed transistors and solar cells

*Amaia Diaz de Zerio Mendaza, Armantas Melianas, Stephan Rossbauer, Olof Bäcke, Lars Nordstierna, Paul Erhart, Eva Olsson, Thomas D. Anthopoulos, Olle Inganäs, and Christian Müller**

Amaia Diaz de Zerio Mendaza, Dr. Lars Nordstierna, Dr. Christian Müller

Department of Chemistry and Chemical Engineering, Chalmers University of Technology, 41296 Göteborg, Sweden

*christian.muller@chalmers.se

Armantas Melianas, Prof. Olle Inganäs

Department of Physics, Chemistry and Biology, Linköping University, 58183 Linköping, Sweden

Stephan Rossbauer, Thomas D. Anthopoulos

Department of Physics and Center for Plastic Electronics, Imperial College London, SW7 2BW London, UK

Olof Bäcke, Dr. Paul Erhart, Prof. Eva Olsson

Department of Applied Physics, Chalmers University of Technology, 41296 Göteborg, Sweden

Keywords: fullerenes, solubility, configurational entropy, field-effect transistors, organic solar cells

Fullerenes are an intriguing class of organic semiconductors that feature a high electron affinity and exceptional charge transport properties, desirable for a number of thin-film opto-electronic applications such as field-effect transistors (FETs) and organic solar cells. Despite their desirable solid-state properties a major disadvantage of pristine $C_{60}$ and $C_{70}$ is the seemingly poor solubility in organic solvents,[1, 2] which however can be substantially improved by attaching exohedral moieties to the fullerene cage, albeit at the expense of a high electron mobility.[3-5] In addition, pristine fullerenes suffer from the strong tendency to crystallize during solvent removal, which complicates formation of continuous thin films. As a result, substituted fullerenes, such as in particular phenyl-$C_x$-butyric acid methyl esters (PCBMs; x = 61 or 71), are by far the most widely studied electron acceptor material for organic photovoltaic applications. The trade-off between increased solubility and reduced electron mobility has so far been acceptable for thin-film solar cells because the latter is still sufficiently high to not limit solar cell performance, which more strongly depends on the precise active layer nanostructure. However, as future improvements in device efficiency rely on thick active layers and high-mobility materials,[6] the use of pristine fullerenes may prove to be advantageous provided that solubility issues can be addressed and a favorable nanostructure can be achieved.

The most efficient active layer nanostructure of organic solar cells is the bulk-heterojunction, which is typically prepared by co-processing a fullerene acceptor and a suitable donor from a common organic solvent. Although devices based on the pristine fullerene $C_{70}$ have been reported for both polymer and small-molecule donors with a power-conversion efficiency PCE of 5.1 % and 5.9 %, respectively,[7, 8] the most competitive results are currently achieved with the more soluble PCBMs, which can yield a PCE of more than 10 %.[9] As low cost is the major selling point of organic photovoltaics, it is desirable to choose the most cost-effective materials. In this regard, the use of PCBMs as the electron

acceptor is not optimal. The additional synthesis steps required to prepare these derivatives from pristine fullerenes considerably increase the energy footprint, which implies a higher environmental impact as well as an overall higher materials cost. For instance, Anctil *et al.* calculated a life cycle embodied energy as low as about 8 GJ $kg^{-1}$ for the as-synthesized $C_{60}$:$C_{70}$ mixture, which increases to 25 GJ $kg^{-1}$ for $C_{60}$ and 38 GJ $kg^{-1}$ for $C_{70}$ after separation and electronic-grade purification.[10] In contrast, preparation of substituted fullerenes consumes significantly more energy, i.e. 65 GJ $kg^{-1}$ and 90 GJ $kg^{-1}$ for electronic-grade $PC_{61}BM$ and $PC_{71}BM$, respectively. Therefore, in particular the use of pristine ~~fullerenes and in particular~~ $C_{60}$:$C_{70}$ mixtures may result in significant energy savings and thus a cheaper acceptor material compared to PCBMs but also individual $C_{60}$ or $C_{70}$, provided that the ability to fabricate opto-electronic devices from solution is not impaired.

Gratifyingly, previous studies have shown that the solubility of $C_{60}$ and $C_{70}$ can be strongly enhanced by co-dissolution in a common organic solvent such as styrene, *o*-xylene and *o*-dichlorobenzene (*o*-DCB).[2, 11] In this communication we establish that the observed enhancement in solubility occurs due the high configurational entropy associated with $C_{60}$:$C_{70}$ mixtures, which in addition facilitates the formation of amorphous thin films. Moreover, we demonstrate that this 'entropic dissolution' of $C_{60}$:$C_{70}$ mixtures is an effective strategy that permits to prepare high-performance FETs with an electron-mobility of 1 $cm^2$ $V^{-1}$ $s^{-1}$ as well as highly reproducible polymer solar cells with a PCE of 6% and a thermally stable active layer.

In a first set of experiments we studied the solubility of $C_{60}$ and $C_{70}$ as well as 1:1 $C_{60}$:$C_{70}$ mixtures at 27 ºC in a variety of organic solvents with a wide range of boiling points, including *o*-xylene, *o*-DCB, and 1-chloronaphthalene (Table 1). The solubility was determined by adding an excess of fullerene material to the various solvents, followed by dissolution of the soluble fraction over the course of two days and careful determination of the

concentration after removal of the insoluble fraction by centrifugation (cf. Experimental Section for details). For all investigated solvents we find that the solubility of the 1:1 mixture is significantly enhanced compared to the solubility of either of the pure components in the same solvent. More polar chlorinated solvents gave rise to the highest solubility, reaching 62 g $L^{-1}$ for the high boiling point solvent 1-chloronaphthalene. Intriguingly, we also observed a relatively high solubility of 19 g $L^{-1}$ for *o*-xylene, which opens up the possibility of processing pristine fullerenes from more benign, i.e. less toxic non-chlorinated solvents.

In order to elucidate the origin of the enhanced solubility of pristine fullerene mixtures we carried out a more extended study of the solubility as a function of $C_{60}$:$C_{70}$ ratio with *o*-DCB as the solvent, which is commonly used for device processing. For reference $C_{60}$ and $C_{70}$ we find a solubility of 22 g $L^{-1}$ and 26 g $L^{-1}$, respectively. In contrast, all $C_{60}$:$C_{70}$ mixtures displayed a notable increase in solubility, which reached a broad maximum at 54 g $L^{-1}$ for a 1:1 weight ratio (**Figure 1a**). We explain this observation by the higher configurational entropy of the ternary $C_{60}$:$C_{70}$:*o*-DCB system as compared to the reference $C_x$:*o*-DCB binaries (x=60 or 70). For dilute concentrations of fullerene solutes, which have a finite molecular volume, the entropy gain upon dissolving two instead of one component in a common solvent can be approximated by:

$$\Delta S \propto \phi_{C_{60}} \cdot \phi_{C_{70}}, \quad (1)$$

where $\phi_{C_{60}}$ and $\phi_{C_{70}}$ are the volume fractions of $C_{60}$ and $C_{70}$, respectively (see Supporting Information for the derivation of equation 1). According to equation 1 the highest entropy gain and thus solubility can be anticipated for a 1:1 volume ratio, i.e. $\phi_{C_{60}} = \phi_{C_{70}}$. Adams *et al.*[12, 13] have calculated a van der Waals molecular volume $V_{vdW}$ of 549 $Å^3$ for $C_{60}$ and 646 $Å^3$ for $C_{70}$. Comparison with the molar masses $M$ of the two fullerenes suggests a close to identical molecular mass density $\rho = M/V_{vdW}$ , i.e. $\rho_{C_{60}} \sim \rho_{C_{70}} \sim 1.3$ g $mol^{-1}$ $Å^{-3}$, and therefore a 1:1 $C_{60}$:$C_{70}$ volume ratio corresponds to a 1:1 $C_{60}$:$C_{70}$ weight ratio. Strikingly, we

indeed observe that the maximum solubility for the investigated ternary solutions is centered at a 1:1 $C_{60}$:$C_{70}$ weight ratio. The ternary phase diagram displayed in Figure 1b summarizes the solubility-composition dependence of the $C_{60}$:$C_{70}$:*o*-DCB system: (1) a single-phase region at concentrations above the liquidus line, which yields homogeneous solutions (Figure 1b; region A), and (2) a two-phase region, which is characterized by saturated solutions and aggregates of excess fullerene material (Figure 1b; region B).

In order to investigate the quality of pristine fullerene solutions in more detail we carried out diffusion measurements by pulsed gradient $^{13}$C-NMR spectroscopy. For $C_x$:*o*-DCB binary solutions with a concentration of 10 and 20 g $L^{-1}$ we find a self-diffusion coefficient *D* of $3.9 \cdot 10^{-10}$ $m^2$ $s^{-1}$ for $C_{60}$ and $3.7 \cdot 10^{-10}$ $m^2$ $s^{-1}$ for $C_{70}$ (see Supporting Information, Figure S1). These values are in good agreement with the self-diffusion coefficients that can be expected for molecules with a spherical ($C_{60}$) or prolate ($C_{70}$) geometry according to the Stokes-Einstein relation, which predicts values within ± 20 % of the experimental results depending on the selected boundary conditions (see Supporting Information for details). We thus conclude that in the binary solutions the pristine fullerenes are molecularly dissolved. For ternary solutions we were able to extract the individual self-diffusion coefficients of both $C_{60}$ and $C_{70}$ at concentrations below as well as above the solubility limit of the individual components (cf. Figure 1). Below the solubility limit we observe good agreement between binary and ternary solutions for a low concentration of 10 g $L^{-1}$, indicating that $C_{60}$ and $C_{70}$ tend to remain molecularly dissolved upon mixing. For higher concentrations of 20, 35 and 50 g $L^{-1}$ a slight deviation of no more than 10 % is observed from values that are predicted for solid spheres. This slight decrease in diffusivity may arise from the formation of minor fractions of aggregates of 2, 3, 4, *etc.* fullerene molecules, which would comprise 19 %, 11 %, 9 %, *etc.* of the $C_{60}$:$C_{70}$ mixture (see Supporting Information for details). Therefore, we

conclude that a fine, close-to-molecular distribution is maintained in $C_{60}$:$C_{70}$:*o*-DCB ternary solutions even above the solubility limit of $C_{60}$:*o*-DCB and $C_{70}$:*o*-DCB binaries.

In order to examine the suitability of the here investigated fullerene mixtures as n-type semiconductor materials, we studied the impact of their mixing on electron transport. To this end we prepared bottom-gate, top-contact (BG-TC) field-effect transistors (FETs). Devices were fabricated by spin-coating *o*-DCB solutions of pristine fullerenes, to which we added about 9 wt% ultra-high molecular weight polystyrene (UHMW-PS) as a binder to ease film formation.[14] Remarkably, reference films based on either $C_{60}$ or $C_{70}$ dewet during spin-coating, whereas the use of $C_{60}$:$C_{70}$ mixtures resulted in even film coverage (**Figure 2a**). This observation may be explained by the reduced tendency of fullerenes to crystallize upon mixing, which is well documented for substituted fullerenes (PCBMs) and leads to the formation of disordered thin films.[15-17] We note that as a result of improved film formation FETs based on fullerene mixtures allow for greater reproducibility. The FET device characteristics are largely independent of the fullerene ratio with a threshold voltage $V_{th}$ ~ 6-7 V and an ON-OFF ratio of $10^5$ (see Figure 2b,c for transfer and output characteristics). We extract a saturated electron mobility of $\mu_e$ ~ 1 $cm^2\ V^{-1}\ s^{-1}$ that is independent of the $C_{60}$:$C_{70}$ ratio (Figure 2d). Evidently, the here investigated fullerene mixtures feature excellent charge transport properties, which are on par with results reported for solution-processed pristine fullerenes.[5, 18] It is worth noting that the absence of ordered domains (see Supporting Information Figure S2), combined with the high symmetry of the fullerene molecules, implies several attractive features such as the absence of grain boundaries, which can impede charge transport, as well as isotropic device characteristics.[19]

We further explored the use of pristine fullerene mixtures as an acceptor material for polymer solar cells. Devices were fabricated with standard geometry (see inset **Figure 3a**) using a widely studied narrow-bandgap fluorothieno-benzodithiophene copolymer (PTB7) as

the donor material.[20-22] Active layers were prepared by first co-dissolving PTB7 with mixtures of pristine fullerenes in *o*-DCB, using concentrations of 30-40 g $L^{-1}$, followed by spin-coating to form ~ 90-150 nm thin films (see Experimental Section for details).

Initially, we investigated the influence of the polymer:fullerene stoichiometry (using a fixed 1:1 $C_{60}$:$C_{70}$ ratio) and found that equal amounts of donor and acceptor material resulted in solar cells with the highest performance (Supporting Information, Figure S3). Therefore, for all remaining experiments we used a 1:1 PTB7:fullerene stoichiometry but varied the $C_{60}$:$C_{70}$ ratio. While all 1:1 PTB7:fullerene photovoltaic devices display a similarly high fill factor *FF* ~ 0.6 and an open-circuit voltage $V_{oc}$ ~ 0.66 V, the short-circuit current density $J_{sc}$ varied more strongly with $C_{60}$:$C_{70}$ ratio. The PTB7:$C_{60}$ binary mixture delivered the lowest $J_{sc}$ ~ 11.9 mA $cm^{-2}$ (Figure 2a), which we ascribe to the weaker absorption of $C_{60}$ as compared to $C_{70}$ across the 360-650 nm region.[11] This observation is supported by the corresponding external quantum efficiency (EQE) spectra (Figure 2b), which confirm that the replacement of $C_{60}$ by $C_{70}$ allows for larger photocurrent generation in the 360-650 nm region. In fact a $J_{sc}$ as high as 14.9 mA $cm^{-2}$ is achieved for 2:1:1 PTB7:$C_{60}$:$C_{70}$, which is comparable to PTB7:$PC_{71}BM$ solar cells with a similar device architecture.[20, 21] The higher *FF* reported by Lu *et al.* was obtained with a higher molecular-weight PTB7 ($M_n$ ~ 128 kg $mol^{-1}$), which led to a considerable increase in the PCE of PTB7:$PC_{71}BM$ based solar cells.[21] We therefore propose that the here observed *FF* ~ 0.6 is not an inherent limitation of the pristine fullerene mixture itself, as corroborated by the high field-effect electron mobilities, discussed in the previous section, but mostly due to the lower molecular weight of the PTB7 used in this study ($M_n$ ~ 34 kg $mol^{-1}$).

We find that the open-circuit voltage $V_{oc}$ ~ 0.66 V is independent of the fullerene ratio (see Figure 3a and Table 2). The use of pristine fullerenes leads to a ~ 0.1 V reduction in $V_{oc}$ as compared to PCBM-based devices.[21] This observation consistent with our previous

work on solar cells based on a thiophene-quinoxaline copolymer (TQ1),[11, 23] and thus we propose that further optimization of polymer solar cells based on $C_{60}$:$C_{70}$ mixtures may require the selection of alternative donor materials that are specifically designed for use with pristine fullerenes. To understand whether the open-circuit voltage of PTB7:$C_{60}$:$C_{70}$ based solar cells is inherently limited by our choice of materials we carried out a more detailed investigation. We rely on the empirical rule that the $V_{oc}$ of organic solar cells is directly related to the energy of the charge-transfer (CT) state $E_{CT}$, which we estimate by fitting the lower energy part of Fourier-transform photocurrent spectroscopy (FTPS) spectra, which originates from an excitation in the CT manifold.[24, 25] We find an $E_{CT}$ ~ 1.26 eV that is largely unaffected by the fullerene ratio (Figure 3c), which is consistent with our observation that the $C_{60}$:$C_{70}$ ratio does not affect the open-circuit voltage of the corresponding solar cells. We thus conclude that the open-circuit voltage obtained with the here investigated PTB7:$C_{60}$:$C_{70}$ ternary blends is inherently limited by the choice of materials, i.e. a $V_{oc}$ ~ 0.66 V is likely the upper limit for optimized photovoltaic devices based on PTB7 and pristine fullerenes.

Overall, we obtained a PCE of 4.9 % for devices based on $C_{60}$, whereas devices based on $C_{70}$ or the mixture $C_{60}$:$C_{70}$ yielded a PCE of 6 %, with champion solar cells of 6.5% for the ternary blend (Table 2). Since the $C_{60}$:$C_{70}$ ratio that is obtained during fullerene synthesis can range from 4:1 to about 4:3.2, depending on the preparation route,[10, 11] we also tested 5:4:1 PTB7:$C_{60}$:$C_{70}$ devices, which yielded a comparably high PCE of 5.1%. To the best of our knowledge, these are the highest reported PCE values for a polymer solar cell employing pristine fullerenes as the acceptor. Moreover, we find that solar cells based on PTB7:$C_{60}$:$C_{70}$ are highly reproducible, as evidenced by a comparison of a total of 36 devices (Figure 3d), and thermally stable, which we tested by annealing the active layer for 10 min at 100 $^{o}$C prior to the deposition of the top electrode (see Table 2). Certainly, both of these properties

are highly desirable for the future upscaling of organic photovoltaic technology.

In order to examine the nanostructure of the here investigated active layer blends in more detail we carried out transmission electron microscopy (TEM) and photoluminescence (PL) spectroscopy. To this end, we spin-coated thin films from *o*-DCB solutions with a total materials content of 30 g $L^{-1}$, which also yielded some of the most efficient solar cells (cf. Table 2). Whereas for this concentration the solubility limit of $C_{60}$ has been reached, $C_{70}$ remains mostly soluble (cf. Figure 1). Instead, for $C_{60}$:$C_{70}$ ratios ranging from 4:1 to 1:4 full solubility can be anticipated. Independent of the $C_{60}$:$C_{70}$ ratio, TEM images indicate a fine-grained/homogeneous nanostructure and the absence of fullerene crystals, as corroborated by the corresponding electron diffraction patterns, which only feature a broad, amorphous halo (Supporting Information, Figure S4). The fine-grained nanostructure is further corroborated by PL spectroscopy. The efficiency of excitation quenching can be defined by the PL quenching ratio Ψ, i.e. the ratio of the integrated PL spectra of neat PTB7 and the PTB7:fullerene blend (see Experimental Section). For 1:1 PTB7:$C_{60}$ we determine a PL quenching ratio of $\Psi \sim 150$, which indicates a well-intermixed nanostructure of this binary blend (Supporting Information, Table S1). Instead, for ternary blends with a $C_{60}$:$C_{70}$ ratio between 4:1 and 1:4 as well as for 1:1 PTB7:$C_{70}$ we observe significantly higher values of $\Psi > 240$, which suggest an even finer distribution of the fullerene acceptor material for these more soluble blend ratios. Evidently, pristine fullerenes and in particular fullerene mixtures can be used as the electron acceptor material in polymer:fullerene bulk-heterojunction blends without causing any apparent phase separation, in agreement with the high EQEs and short-circuit current densities of the corresponding photovoltaic devices.

Finally, we argue that the concept of 'entropic dissolution' is applicable to other organic semiconductor mixtures. In order to substantiate this claim we carried out a final set of experiments to investigate the solubility of one very different system based on rubrene

and 5,12-diphenylanthracene (DPA) in toluene at 27 ºC, which Stingelin et al. have employed to spin-coat glassy films that can be carefully crystallized through thermal annealing to form the active layer of FETs.[14] We observe a substantial increase in solubility with a maximum at a weight ratio of about 1:2 rubrene:DPA (Supporting Information, Figure S5), which coincides with the range of compositions that display the highest tendency to vitrify (cf. Ref. [14]). In contrast to $C_{60}$:$C_{70}$ the maximum solubility does not occur at a 1:1 weight or volume ratio, indicating that besides the configurational entropy of mixing also differences in the conformational entropy of rubrene and DPA as well as, potentially, molecular interactions must be considered. We conclude that judicious co-dissolution of organic semiconductor mixtures is a general approach that can be used to enhance the solubility and, in addition, is highly relevant for designing optimal processing schemes for, e.g., glass-forming alloys.

**Supporting Information**

Supporting Information including experimental details is available from the Wiley Online Library or from the authors.

**Acknowledgements**

Financial support from the Swedish Research Council, Formas, the Chalmers Area of Advance Energy, the Knut and Alice Wallenberg Foundation through two Wallenberg Academy Fellowships, and the European Research Council (ERC) under grant agreement no. 637624 is gratefully acknowledged.

Received: ((will be filled in by the editorial staff))
Revised: ((will be filled in by the editorial staff))
Published online: ((will be filled in by the editorial staff))

[1] R. J. Doome, S. Dermaut, A. Fonseca, M. Hammida, J. B. Nagy, *Fullerene Sci. Technol.* **1997**, *5*, 1593.

[2] K. N. Semenov, N. A. Charykov, V. A. Keskinov, A. K. Piartman, A. A. Blokhin, A. A. Kopyrin, *J. Chem. Eng. Data* **2010**, *55*, 13.

[3] P. H. Wöbkenberg, D. D. C. Bradley, D. Kronholm, J. C. Hummelen, D. M. de Leeuw, M. Cölle, T. D. Anthopoulos, *Synth. Met.* **2008**, *158*, 468.

[4] R. C. I. MacKenzie, J. M. Frost, J. Nelson, *J. Chem. Phys.* **2010**, *132*, 064904.

[5] S. Rossbauer, C. Müller, T. D. Anthopoulos, *Adv. Funct. Mater.* **2014**, *24*, 7116.

[6] S. Foster, F. Deledalle, A. Mitani, T. Kimura, K. B. Kim, T. Okachi, T. Kirchartz, J. Oguma, K. Miyake, J. R. Durrant, S. J. Doi, J. Nelson, *Adv. Energy Mater.* **2014**, *4*, 1400311.

[7] K. Tada, *Sol. Energy Mater. Sol. Cells* **2015**, *143*, 52.

[8] H. W. Lin, J. H. Chang, W. C. Huang, Y. T. Lin, L. Y. Lin, F. Lin, K. T. Wong, H. F. Wang, R. M. Ho, H. F. Meng, *J. Mater. Chem. A* **2014**, *2*, 3709.

[9] Y. H. Liu, J. B. Zhao, Z. K. Li, C. Mu, W. Ma, H. W. Hu, K. Jiang, H. R. Lin, H. Ade, H. Yan, *Nat. Commun.* **2014**, *5*, 8.

[10] A. Anctil, C. W. Babbitt, R. P. Raffaelle, B. J. Landi, *Environ. Sci. Technol.* **2011**, *45*, 2353.

[11] A. Diaz De Zerio Mendaza, J. Bergqvist, O. Bäcke, C. Lindqvist, R. Kroon, F. Gao, M. R. Andersson, E. Olsson, O. Inganäs, C. Müller, *J. Mater. Chem. A* **2014**, *2*, 14354.

[12] G. B. Adams, M. Okeeffe, R. S. Ruoff, *J. Phys. Chem.* **1994**, *98*, 9465.

[13] R. Haselmeier, M. Holz, M. M. Kappes, R. H. Michel, D. Fuchs, *Phys. Chem. Chem. Phys.* **1994**, *98*, 878.

[14] N. Stingelin-Stutzmann, E. Smits, H. Wondergem, C. Tanase, P. Blom, P. Smith, D. De Leeuw, *Nat. Mater.* **2005**, *4*, 601.

[15] C. Lindqvist, J. Bergqvist, O. Bäcke, S. Gustafsson, E. Wang, E. Olsson, O. Ingänas, M. R. Andersson, C. Müller, *Appl. Phys. Lett.* **2014**, *104*, 153301.

[16] B. C. Schroeder, Z. Li, M. A. Brady, G. C. Faria, R. S. Ashraf, C. J. Takacs, J. S. Cowart, D. T. Duong, K. H. Chiu, C. H. Tan, J. T. Cabral, A. Salleo, M. L. Chabinyc, J. R. Durrant, I. McCulloch, *Angew. Chem. Int. Ed.* **2014**, *53*, 12870.

[17] D. Angmo, M. Bjerring, N. C. Nielsen, B. C. Thompson, F. C. Krebs, *J. Mater. Chem. C* **2015**, *3*, 5541.

[18] W. Kang, M. Kitamura, Y. Arakawa, *Org. Electron.* **2013**, *14*, 644.

[19] P. J. Skabara, J. B. Arlin, Y. H. Geerts, *Adv. Mater.* **2013**, *25*, 1948.

[20] Y. Y. Liang, Z. Xu, J. B. Xia, S. T. Tsai, Y. Wu, G. Li, C. Ray, L. P. Yu, *Adv. Mater.* **2010**, *22*, E135.

[21] L. Y. Lu, L. P. Yu, *Adv. Mater.* **2014**, *26*, 4413.

[22] C. Liu, C. Yi, K. Wang, Y. L. Yang, R. S. Bhatta, M. Tsige, S. Y. Xiao, X. Gong, *ACS Appl. Mater. Interfaces* **2015**, *7*, 4928.

[23] C. Lindqvist, J. Bergqvist, C. C. Feng, S. Gustafsson, O. Bäcke, N. D. Treat, C. Bounioux, P. Henriksson, R. Kroon, E. G. Wang, A. Sanz-Velasco, P. M. Kristiansen, N. Stingelin, E. Olsson, O. Inganäs, M. R. Andersson, C. Müller, *Adv. Energy Mater.* **2014**, *4*, 1301437.

[24] K. Vandewal, K. Tvingstedt, A. Gadisa, O. Inganäs, J. V. Manca, *Phys. Rev. B* **2010**, *81*, 125204.

[25] K. Vandewal, K. Tvingstedt, J. V. Manca, O. Inganäs, *IEEE J. Sel. Top. Quantum Electron.* **2010**, *16*, 1676.

[26] R. S. Ruoff, D. S. Tse, R. Malhotra, D. C. Lorents, *J. Phys. Chem.* **1993**, *97*, 3379.

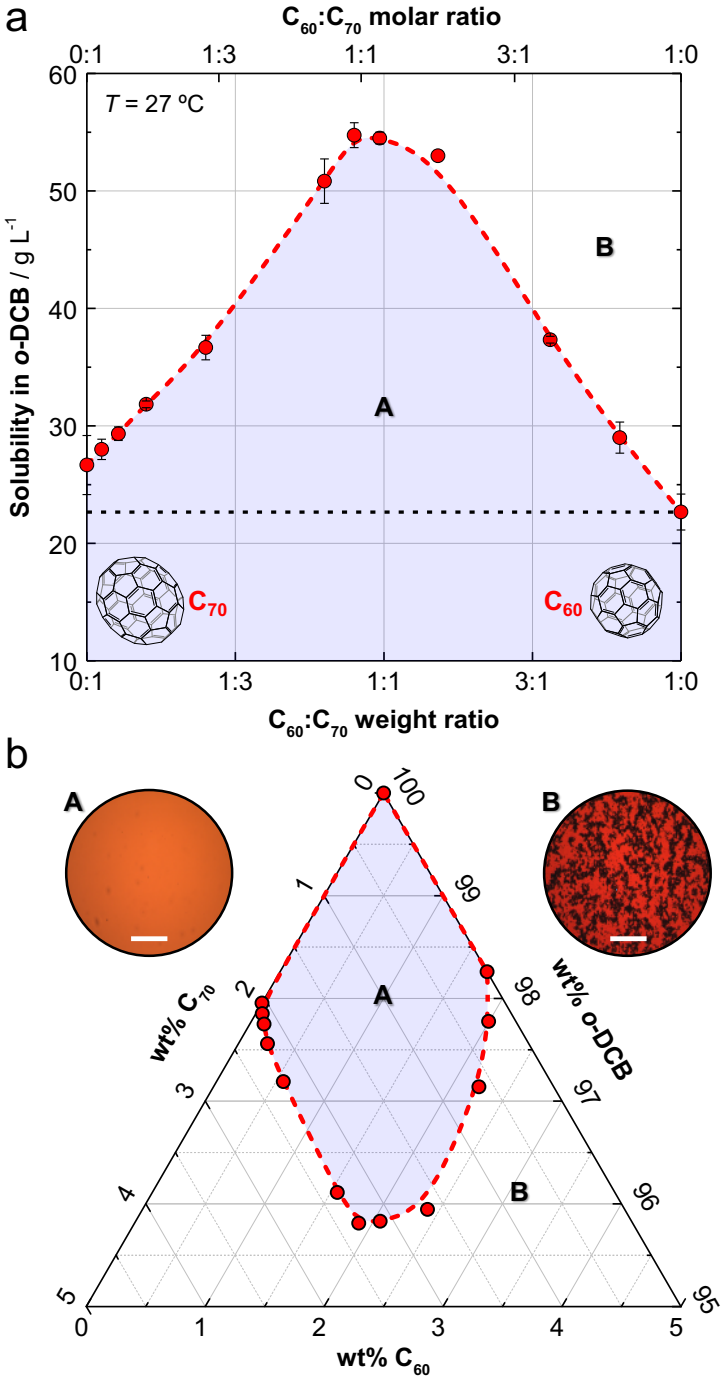


**Figure 1.** (**a**) Solubility of $C_{60}$ and $C_{70}$ in *o*-DCB at 27 °C as a function of $C_{60}$:$C_{70}$ weight ratio (molar ratio). (**b**) Ternary phase diagram for $C_{60}$:$C_{70}$:*o*-DCB at 27 °C, showing (A) a single phase region (blue-shaded area) and (B) a two phase region; transmission optical micrographs of a 35 g $L^{-1}$ solution of 1:1 $C_{60}$:$C_{70}$ (top left) and 60 g $L^{-1}$ solution of 3:1 $C_{60}$:$C_{70}$ (top right),

sandwiched between glass slides, reveal the appearance of aggregates in the two phase region (scale bars 300 µm).

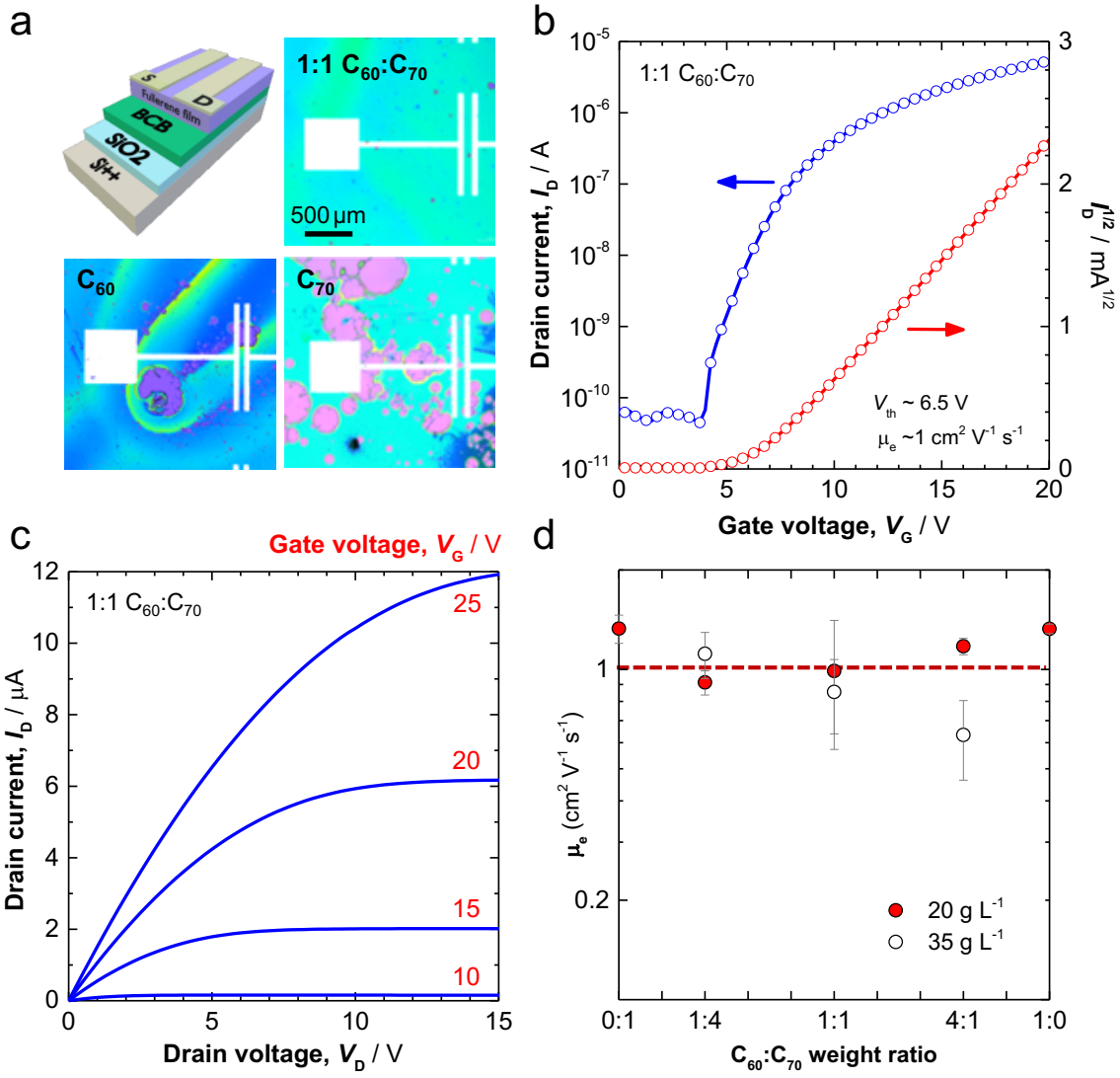


**Figure 2.** (**a**) Schematic representation of the bottom-gate, top-contact (BG-TC) transistor architecture and optical micrographs of fullerene films on the transistor test substrates. Note the complete coverage of 1:1 $C_{60}$:$C_{70}$ films, whereas $C_{60}$ and $C_{70}$ films ruptured leading to circular defects. (**b**) FET transfer (Drain voltage $V_D$ = 25 V) and (**c**) output characteristics for a 1:1 $C_{60}$:$C_{70}$ device. The dimensions of the transistor channel were $W$ = 1000 µm and $L$ = 40 µm. (**d**) Saturation mobility as a function of $C_{60}$:$C_{70}$ weight ratio: 35 g $L^{-1}$ (white circles) and 20 g $L^{-1}$ solution of $C_{60}$:$C_{70}$ (red circles).

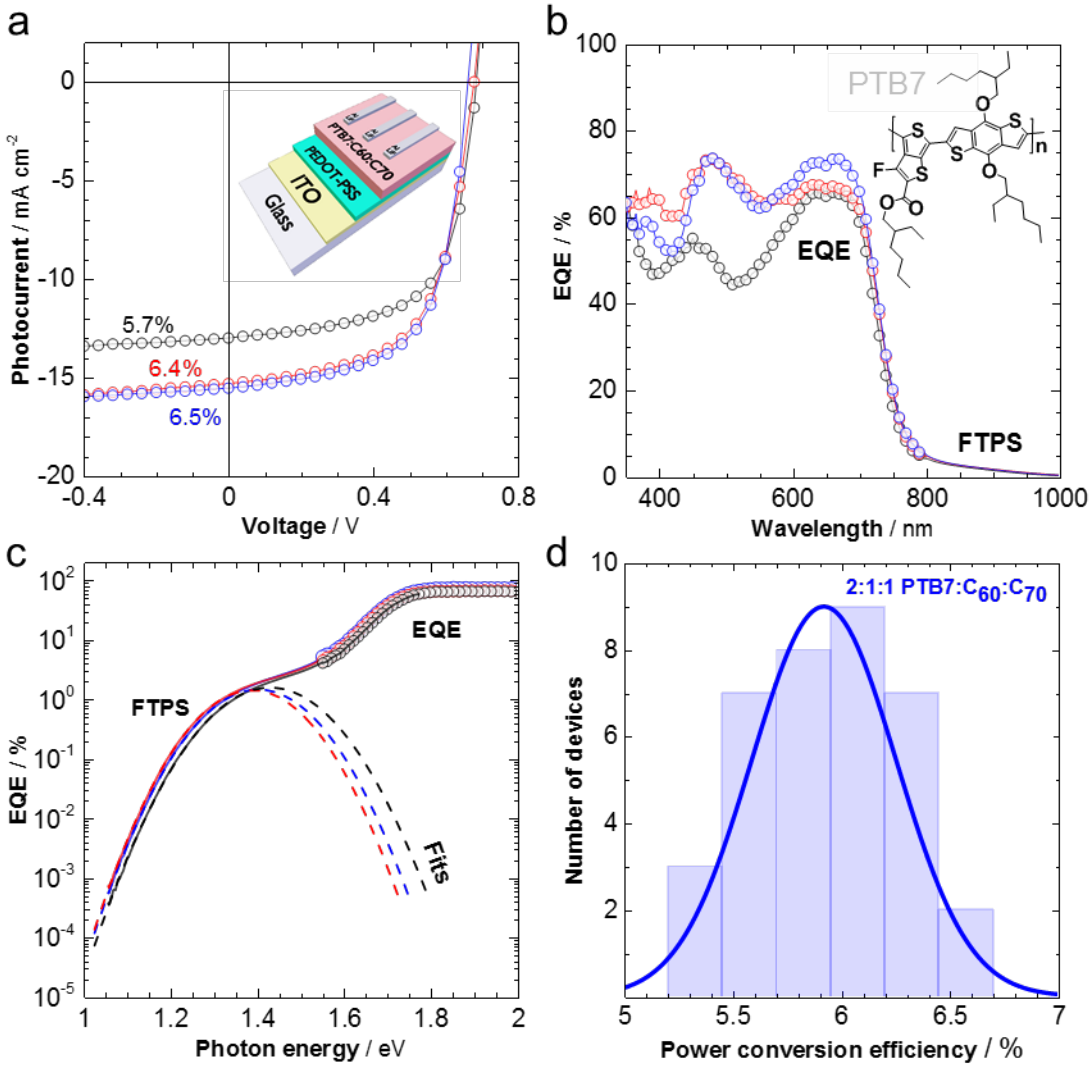


**Figure 3.** (**a**) Current-voltage *J-V* characteristics of 2:1:1 PTB7:$C_{60}$:$C_{70}$ (blue), 1:1 PTB7:$C_{70}$ (red) and 1:1 PTB7:$C_{60}$ (black) based devices. Inset: solar cell device architecture. (**b**) External quantum-efficiency (EQE) spectra corresponding to the devices in panel a. Inset: chemical structure of PTB7. (**c**) Charge-transfer (CT) state studies by Fourier-transform photocurrent spectroscopy (FTPS), i.e. a sensitive measurement of the EQE of the same devices as shown in panels a and b (solid lines). Open circles are the EQE spectra from panel b. Dashed lines are fits according to Marcus theory as suggested by Refs. [24] and [25] from which the energy of the CT state was estimated. (**d**) Device reproducibility of 36 PTB7:$C_{60}$:$C_{70}$ based solar cells; the solid line is a Gaussian fit.

**Table 1.** Solubility of $C_{60}$, $C_{70}$ and 1:1 $C_{60}$:$C_{70}$ mixtures by weight in various organic solvents at 27 ºC; literature values are given where available.

| **Solvent** | **chemical structure** | **boiling point** / ºC | **fullerene solute** | **measured solubility at 27 ºC** / g $L^{-1}$ | **solubility at 25 ºC from Refs. [2, 26]** / g $L^{-1}$ |
|---|---|---|---|---|---|
| toluene | 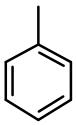 | 111 | $C_{60}$ | 1.0 ± 0.5 | 2.4 |
| | | | $C_{70}$ | 1.3 ± 0.8 | 1.4 |
| | | | $C_{60}$:$C_{70}$ | 2.3 ± 1.2 | - |
| *o*-xylene | 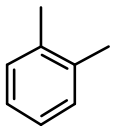 | 144 | $C_{60}$ | 12.8 ± 4.9 | 9.5 |
| | | | $C_{70}$ | 13.5 ± 3.9 | 15.6 |
| | | | $C_{60}$:$C_{70}$ | 18.6 ± 3.2 | ~20 |
| *o*-DCB | 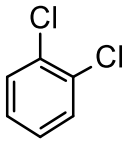 | 180 | $C_{60}$ | 22.6 ± 1.5 | 22.9 |
| | | | $C_{70}$ | 26.6 ± 2.5 | 29.6 |
| | | | $C_{60}$:$C_{70}$ | 54.7 ± 1.1 | - |
| CB | 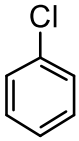 | 131 | $C_{60}$ | 5.7 ± 0.2 | 6.4 |
| | | | $C_{70}$ | 2.1 ± 0.1 | - |
| | | | $C_{60}$:$C_{70}$ | 10.3 ± 0.3 | - |
| 1-chloronaphthalene | 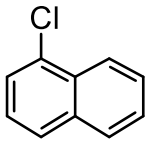 | 263 | $C_{60}$ | 37.5 ± 1.3 | 51.3 |
| | | | $C_{70}$ | 43.6 ± 0.2 | - |
| | | | $C_{60}$:$C_{70}$ | 62.6 ± 0.8 | - |
| carbon disulfide | 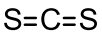 | 46 | $C_{60}$ | 3.2 ± 0.3 | 7.9 |
| | | | $C_{70}$ | 9.6 ± 1.2 | 10.1 |
| | | | $C_{60}$:$C_{70}$ | 12.2 ± 1.0 | - |
| anisol | 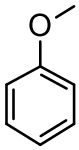 | 154 | $C_{60}$ | 4.1 ± 0.2 | 5.6 |
| | | | $C_{70}$ | 2.5 ± 0.1 | - |
| | | | $C_{60}$:$C_{70}$ | 7.4 ± 0.1 | - |
| 2-methyl thiophene | 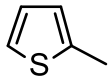 | 113 | $C_{60}$ | 5.3 ± 2.5 | 6.8 |
| | | | $C_{70}$ | 4.3 ± 0.3 | - |
| | | | $C_{60}$:$C_{70}$ | 13 ± 0.9 | - |

**Table 2.** Performance of optimized solar cells: total concentration of solid material in *o*-DCB prior to spin-coating, number of measured devices, thickness of the active layer, short-circuit current density $J_{sc}$, open-circuit voltage $V_{oc}$, fill factor *FF* and power-conversion efficiency PCE (champion results in brackets).

| **Blend** | **Total conc.** / g $L^{-1}$ | **No. of devices** | **Thickness** / nm | $J_{sc}$ / mA $cm^{-2}$ | $V_{oc}$ / mV | *FF* / - | **PCE** / % |
|---|---|---|---|---|---|---|---|
| 1:1 PTB7:$C_{60}$ | 40 | 6 | ~ 90 | 11.9±1.2 | 668±1 | 0.61±0.03 | 4.9±0.6 **(5.7)** |
| 1:1 PTB7:$C_{70}$ | 40 | 6 | ~ 90 | 14.6±0.6 | 664±1 | 0.62±0.01 | 6.0±0.3 **(6.4)** |
| 5:4:1 PTB7:$C_{60}$:$C_{70}$ | 40 | 6 | ~ 120 | 14.3±0.6 | 663±1 | 0.53±0.01 | 5.1±0.3 **(5.4)** |
| 2:1:1 PTB7:$C_{60}$:$C_{70}$ | 40 | 6 | ~ 150 | 14.4±0.7 | 663±1 | 0.62±0.01 | 6.0±0.3 **(6.5)** |
| 2:1:1 PTB7:$C_{60}$:$C_{70}$ | 30 | 24 | ~ 120 | 14.9±0.8 | 660±1 | 0.60±0.03 | 5.9±0.6 **(6.5)** |
| 2:1:1 PTB7:$C_{60}$:$C_{70}$* | 30 | 6 | ~ 120 | 14.1±0.1 | 663±1 | 0.62±0.01 | 5.9±0.3 (**6.2**) |

*annealed for 10 min at 100 °C

**Table of contents**

**The solubility of pristine fullerenes** can be enhanced by mixing $C_{60}$ and $C_{70}$ due to the associated increase in configurational entropy. This 'entropic dissolution' allows to prepare field-effect transistors with an electron mobility of 1 $cm^2 V^{-1} s^{-1}$ and polymer solar cells with a highly reproducible power-conversion efficiency of 6 % as well as a thermally stable active layer.

Keywords: fullerenes, solubility, configurational entropy, field-effect transistors, organic solar cells

A. Diaz de Zerio Mendaza, A. Melianas, S. Rossbauer, O. Bäcke, L. Nordstierna, P. Erhart, E. Olsson, T. D. Anthopoulos, O. Inganäs, C. Müller*

**High-entropy mixtures of pristine fullerenes for solution-processed transistors and solar cells**